Review

Neuronal Networks in Alzheimer's Disease

Yong He, Zhang Chen, Gaolang Gong, and Alan Evans

Alzheimer's disease (AD) is a progressive, neurodegenerative disease that can be clinically characterized by impaired memory and many other cognitive functions. Previous studies have demonstrated that the impairment is accompanied by not only regional brain abnormalities but also changes in neuronal connectivity between anatomically distinct brain regions. Specifically, using neurophysiological and neuroimaging techniques as well as advanced graph theory–based computational approaches, several recent studies have suggested that AD patients have disruptive neuronal integrity in large-scale structural and functional brain systems underlying high-level cognition, as demonstrated by a loss of small-world network characteristics. Small world is an attractive model for the description of complex brain networks because it can support both segregated and integrated information processing. The altered small-world organization thus reflects aberrant neuronal connectivity in the AD brain that is most likely to explain cognitive deficits caused by this disease. In this review, we will summarize recent advances in the brain network research on AD, focusing mainly on the large-scale structural and functional descriptions. The literature reviewed here suggests that AD patients are associated with integrative abnormalities in the distributed neuronal networks, which could provide new insights into the disease mechanism in AD and help us to uncover an imaging-based biomarker for the diagnosis and monitoring of the disease.

Keywords: small-world networks; connectivity; graph theory; cortical thickness; default mode; fMRI; tractography

Alzheimer's disease (AD) is the most common type of dementia, accounting for between 50% and 70% of all cases (Kukull and Bowen 2002). Over the past several decades, there is considerable evidence indicating that patients diagnosed with AD exhibit significant impairments in multiple cognitive domains such as memory, executive functioning, attention, visuospatial skill, and verbal ability. Earlier studies have suggested that these impairments could arise from focal abnormalities in individual brain regions such as the medial temporal structures and posterior (and some frontal) associative cortices (for reviews, see Dickerson and Sperling 2005; Salmon and others 2008). In contrast, recent multidisciplinary researches in neuropathology, electrophysiology, and neuroimaging have suggested that AD patients are associated with structural and functional disruptions in the relationship between anatomically distinct brain regions, which supports the notion of AD as a disconnection syndrome (for a review, see Delbeuck and others 2003; Morrison and others 1986). Specifically, several recent neurophysiological and neuroimaging studies (He, Chen, and Evans 2008; Stam and others 2009; Stam and others 2007; Supekar and others 2008) have used advanced graph theoretical network analysis approaches (Boccaletti and others 2006; Watts and Strogatz 1998) to show that AD patients have disruptive neuronal integrity in large-scale structural and functional brain systems underlying high-level cognitive functions (Table 1). For instance, these studies have consistently demonstrated that AD patients exhibit abnormal segregated and integrative connectivity patterns as characterized by a loss of small-world network characteristics. The small-world model (Fig. 1) (Watts and Strogatz 1998) is attractive for the characterization of complex brain networks because it captures both segregated and integrated information processing of the brain (Bassett and Bullmore 2006; Stam and Reijneveld 2007). Thus, these new emerging concepts have revolutionized the previous view of the AD-associated brain regional or inter-regional abnormalities by demonstrating disruptive system integrity in large-scale brain networks.

In this review, we will summarize recent advances made in the AD-related brain network research, focusing specifically on the alterations of topological organization in the large-scale structural and functional brain networks revealed by neurophysiological and

333

Table 1. Overview of Large-Scale Functional and Structural Brain Network Studies in Alzheimer's Disease

Study	Population	Imaging Modality	Network Type	Network Size	Connectivity Metrics	Main Findings
Stam and others 2007	AD (N = 15; age, 54–77 y; MMSE, 15–28) NC (N = 13; age, 57–78 y; MMSE, 27–30)	EEG (resting state)	Unweighted brain networks	21 × 21	Synchronization likelihood of regional time courses	1) Unchanged clustering coefficient and longer characteristic path length in the functional brain networks of AD 2) Negative correlation between MMSE scores and path length for all subjects.
Stam and others 2009	AD (N = 18; age, 72.1 ± 5.6 (mean ± SD) y; MMSE, 13–25) NC (N = 18; age, 69.1 ± 6.8 (mean ± SD) y; MMSE, 27–30)	MEG (resting state)	Weighted brain networks	149 × 149	Phase lag index of regional time courses	1) Lower clustering coefficient and higher characteristic path length in the functional brain networks (8–10 Hz) of AD 2) Lower normalized clustering coefficient and lower normalized characteristic path length in the functional brain networks (8–10 Hz) of AD 3) Positive correlation between MMSE scores and normalized clustering coefficients for all subjects.
Supekar and others 2008	AD (N = 21; age, 48–83 y; MMSE, 12–29) NC (N = 18; age, 37–77 y; MMSE, 27–30)	Functional MRI (resting state)	Unweighted brain networks	90 × 90	Wavelet correlation of regional time courses	1) Lower clustering coefficient and unchanged characteristic path length in the functional brain networks of AD 2) Lower clustering in the left and right hippocampus in AD.
He and others 2008	AD (N = 92; age, 62–96 y; MMSE, 14–30) NC (N = 97; age, 60–94 y; MMSE, 25–30)	Structural MRI	Unweighted brain networks	54 × 54	Partial correlation of regional cortical thickness	1) Higher clustering coefficient and longer characteristic path length in the structural brain networks of AD 2) Decreased topological centrality in temporal and parietal areas and increased centrality in the occipital regions in AD

Note: All studies have consistently demonstrated that AD patients had a loss of small-world network characteristics in the large-scale brain networks. AD = Alzheimer's disease; NC = normal controls; MMSE = Mini Mental State Examination; EEG = electroencephalograph; MEG = magnetoencephalograph; MRI = magnetic resonance imaging.

neuroimaging data using modern graph theoretical approaches. First, some basic concepts regarding brain connectivity and graph theoretical approaches are addressed. Next, we will review the AD-related changes of the brain functional networks observed from electroencephalograph (EEG), magnetoencephalograph (MEG), and functional magnetic resonance imaging (fMRI) data. Then, we will review recent findings of disruptive structural brain connectivity in AD using structural MRI and diffusion MRI techniques. Finally, a future perspective on the studies of neuronal networks in both the healthy and AD populations is discussed.

Basic Concepts

Brain Connectivity Networks

Brain networks can be described at different organizational levels such as single neurons (microscale), a group of neurons (mesoscale), or anatomically distinct brain regions (macroscale or large-scale) (Sporns and others 2005). In this review, we will focus on the examination of the human brain networks at a macroscale.

In a macroscale brain network, one of the most basic elements is the nodes, which can be defined as EEG electrodes (Ferri and others 2007; Micheloyannis,
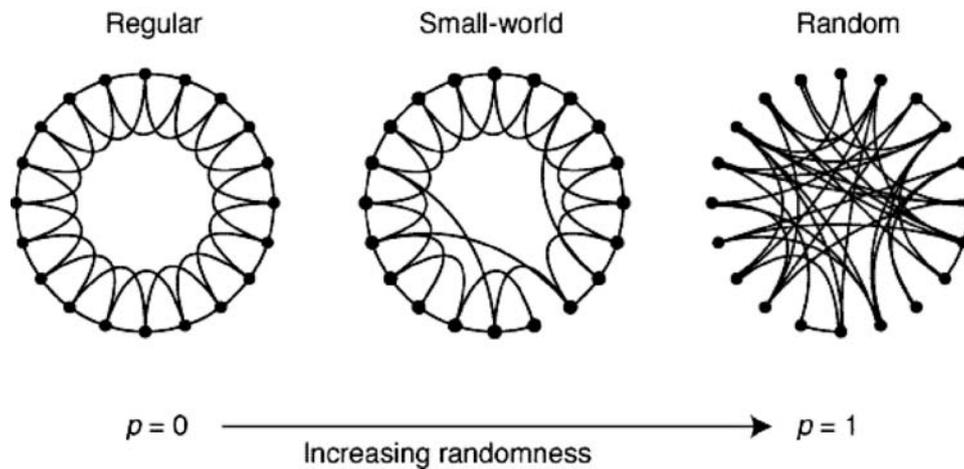
Figure 1. Small-world network (Watts and Strogatz 1998). The authors start with a ring of *n* nodes, each connected to its *k* nearest neighbors by undirected edges. (For clarity, *n* = 20 and *k* = 4 in the schematic examples shown here.) They choose a node and the edge that connects it to its nearest neighbors in a clockwise sense. With a reconnection probability of *p*, they moved the edge to a node chosen uniformly at random over the entire ring, with a restriction on the duplicate edges; otherwise, they leave the edge in place. They repeat this process by moving clockwise around the ring, considering each node in turn until one lap is completed. Next, they consider the edges that connect nodes to their second nearest neighbors clockwise. As in the previous step, they randomly rewire each of these edges with a probability of *p*, repeating this process while circulating around the ring and proceeding outward to more distant neighbors after each lap, until each edge in the original lattice has been considered once. (As there are *nk*/2 edges in the entire graph, the rewiring process stops after *k*/2 laps.) Three realizations of this process are shown for different values of *p*. For *p* = 0, the original ring is unchanged; as *p* increases, the graph becomes increasingly disordered until for *p* = 1, all edges are rewired randomly. One of their main results is that for intermediate values of *p*, the graph is a small-world network: highly clustered like a regular graph, yet with small characteristic path lengths similar to a random graph.

Pachou, Stam, Vourkas, and others 2006; Rubinov and others 2007; Stam and others 2007), MEG channels (Bassett and others 2006; Stam 2004; Stam and others 2009), or regions of interests derived from anatomical atlases in MRI (Bassett and others 2008; Hagmann and others 2008; He, Chen, and Evans 2007; Salvador and others 2005). Another basic network element is the network edges linking the nodes, which can be defined by the functional or structural associations among different neuronal elements of the brain. To date, brain functional associations are measured by either the temporal correlation between spatially remote neurophysiological events, often referred to as the functional connectivity (Friston, Frith, Liddle, and Frackowiak 1993), or the influence that one neural system exerts over another, also referred to as the effective connectivity (Friston, Frith, and Frackowiak 1993). Structural association can be measured by examining the information of structural connections among neuronal elements. In this review, the definition of structural brain connectivity was extended to include 1) true anatomical connectivity that describes the brain white matter bundles linking neuronal units (Sporns and others 2004) in terms of the existence (Gong and others 2009), probability (Iturria-Medina and others 2008), and density (Hagmann and others 2008; Hagmann and others 2007) measures, and 2) morphometric connectivity that represents the statistical interdependencies of morphological features between different brain regions such as the cortical thickness

(Chen and others 2008; He, Chen, and Evans 2008; He, Chen, and Evans 2007), gray matter volumes (Bassett and others 2008; He, Chen, Rosa, and others 2007), density, areas, and complexity. On the basis of these methods, the structural and functional brain networks can be constructed and further characterized by using graph theoretical approaches.

Graph Theoretical Approaches

A complex brain network can be represented as a graph *G* with *N* nodes and *K* edges in which nodes represent brain regions and edges represent connections between brain regions, respectively. A graph whose edges are directed from one node to another is called a directed graph, whereas a graph whose edges have no sense of direction is called an undirected graph. Also, a graph is said to be an unweighted (binary) graph if every edge in the graph has an equal weight of 1, whereas a graph is weighted if its edges are assigned with different strengths. In this review, we will only focus on undirected brain networks. The descriptions for directed graphs can be found in other literature (Bang-Jensen and Gutin 2000; Boccaletti and others 2006).

For an undirected and unweighted graph, its clustering coefficient (C_p) and characteristic path length (L_p) are 2 basic network measurements that are frequently applied to quantify the local and global topological architecture (Boccaletti and others 2006;

Watts and Strogatz 1998). The C_p is the average of the clustering coefficients over all nodes in a network, where the clustering coefficient C_i of a node i is defined as the number of existing connections among the node's neighbors divided by all their possible connections. C_p quantifies the extent of local cliquishness or local efficiency of information transfer of a network (Latora and Marchiori 2001; Watts and Strogatz 1998). The L_p of a network is the average minimum number of connections that link any two nodes of the network. However, this original definition of L_p is problematic in networks that comprise more than one component because there exist nodal pairs that have no connecting path. To avoid this problem, L_p can be measured by using a "harmonic mean" distance between any pairs of network nodes proposed by Newman (2003), that is, the reciprocal of the average of the reciprocals. L_p quantifies the ability of parallel information propagation or global efficiency (in terms of $1/L_p$) of a network (Latora and Marchiori 2001). The two measurements can be used to distinguish different types of networks such as regular, small-world, and random networks (Fig. 1). A regular network tends to have a greater clustering coefficient but a longer characteristic path length due to the lack of long-distance connections, but a random network tends to have a lower clustering coefficient but a smaller characteristic path length. In a small-world network, the nodes usually have greater local interconnectivity or cliquishness than those of a random network, but the minimum path length between any pair of nodes is smaller than would be expected of those of a regular network. Mathematically, a real network would be considered small world if it meets the following conditions: $C_p/C_p^{rand} > 1$ and $L_p/L_p^{rand} \sim 1$ (Watts and Strogatz 1998), where C_p^{rand} and L_p^{rand} are the mean clustering coefficient and characteristic path length of the matched random networks, respectively. These measures can also be extended to describe the topological architecture of weighted graphs by taking into account the connection strengths between nodes (Boccaletti and others 2006). Using these measurements, small-world topology has been recently demonstrated in many complex brain networks in mammalian and human brain (for reviews, see Bassett and Bullmore 2006; Stam and Reijneveld 2007). Small world is an attractive model for the description of complex brain networks because it not only supports both specialized/modularized and integrated/distributed information processing but also maximizes the efficiency of information transfer at a relatively low wiring cost (Bassett and Bullmore 2006; Sporns and others 2004).

In addition to these network parameters, several other metrics can also be applied to describe the nodal characteristics such as degree, efficiency, and betweenness centrality. The degree K_i of a node i is the number of all edges for the node. The nodal efficiency E_i is the inverse of the harmonic mean of the minimum path length between the node i and all other nodes in the network (Achard and Bullmore 2007; Latora and Marchiori 2001). The betweenness B_i of a node i is defined as the number of shortest paths between any two nodes that run through node i (Freeman 1977). These nodal measurements can be used to identify those network hubs.

Functional Brain Networks in AD

Electrophysiological and functional neuroimaging techniques are powerful tools to map brain functional activities under both normal and pathological conditions. In this section, we will review some recent research progresses in analyzing the abnormal functional integrity in the large-scale brain systems of AD by using EEG/MEG and fMRI.

EEG/MEG

EEG and MEG measure the changes in the electromagnetic field related to neuronal activity at a high temporal resolution (milliseconds). To date, EEG/MEG data have also been widely used to investigate the abnormal functional integrity between different brain regions in AD. For instance, many studies have reported that, while comparing with normal controls, AD patients had a loss of functional connectivity (linear and/or nonlinear synchronization) predominantly in the alpha and beta bands under no-task/task conditions (Adler and others 2003; Berendse and others 2000; Besthorn and others 1994; Jelic and others 1996; Knott and others 2000; Koenig and others 2005; Pijnenburg and others 2004; Stam and others 2006; Wada and others 1998). The affected functional pathways included many interhemispheric and intrahemispheric (e.g., frontotemporal, frontoparietal, and temporoparietal) connections. These changes of functional connectivity within specific neuronal networks have been suggested to partly explain the impairment of memory and cognitive functions in AD patients.

Recently, many researchers also applied EEG/MEG techniques in combination with graph theoretical approaches to study large-scale topological organization of the whole-brain networks in both the normal subjects and AD patients. The first graph theoretical network analysis of MEG data was performed by Stam (2004). In his study, the brain activity at 126 MEG channels was recorded in five healthy human subjects under a no-task, eyes-closed condition. The pattern of functional connectivity between all pairs of channels was acquired by using the synchronization likelihood (SL), a measurement of the degree of linear and nonlinear coupling between two time series. The resulting matrix (126×126) was further converted into a binary

(i.e., unweighted) graph in which the connection is 1 if the SL value between two channels was larger than a given threshold and 0 otherwise. This procedure was repeated at several different frequency bands: delta (0.5–4 Hz), theta (4–8 Hz), alpha (8–13 Hz), beta (13–30 Hz), and gamma (30–48 Hz). Using graph theoretical analysis, Stam (2004) found that, from the functional brain activity, patterns at the alpha and beta bands had a regular network configuration, whereas at the low (<8 Hz) and high (>30 Hz) frequency bands, they displayed the features of a "small-world" network with a high local clustering and short path lengths between the channels. Following Stam's work, several recent EEG/MEG studies have also demonstrated such small-world topological organization in the functional connectivity networks of the normal human brain during a no-task state or go-directed tasks (Bassett and others 2006; Ferri and others 2007; Micheloyannis, Pachou, Stam, Breakspear, and others 2006; Rubinov and others 2007; Smit and others 2008; Stam and others 2007). These findings suggest that the brain functional activity patterns, whether they are task related or at resting state, have an optimal balance between functional segregation and integrity.

In two recent elegant EEG/MEG studies conducted by VU University, the Netherlands, using graph theoretical analysis, Stam and his colleagues have demonstrated disruptive system integrity in the whole-brain functional connectivity networks in AD (Table 1). In the first study (Stam and others 2007), they investigated the functional connectivity of the beta band-filtered (13–30 Hz) EEG channels in 15 AD and 13 control subjects during a no-task, eyes-closed state. SLs between all pairwise combinations of 21 EEG channels were calculated (Fig. 2). The resulting synchronization matrices were converted into binary networks by applying an average connectivity degree, $<k>$, threshold, and small-world parameters of the networks (cluster coefficients and path lengths) were further computed. Although both groups showed small-world properties in their brain functional networks (compared to randomly generated networks with preserved degree distribution), the AD patients exhibited longer characteristic path length, L_p, over a wide range of thresholds. There was no significant difference observed in the cluster coefficient, C_p, between the two groups. Furthermore, Stam and his colleagues found a significant negative correlation (Pearson $r = -5.91$, $P = 0.01$) between minimum mental state examination score (MMSE) and network path length of all the subjects. These results suggest a disruption of small-world organization in the brain functional networks in AD.

In their second study (Stam and others 2009), Stam and colleagues used MEG to record brain activity signals also under a no-task, eyes-closed condition in 18 AD and 18 nondemented controls (Fig. 3). They first calculated the synchronization between all pairs of 151 channels at multiple frequency bands (delta [0.5–4 Hz], theta [4–8 Hz], lower alpha [8–10 Hz], upper alpha [10–13 Hz], beta [13–30 Hz], and gamma [30–45 Hz]) using a phase lag index (PLI) that is insensitive to the volume conduction and then obtained a PLI-weighted functional connectivity network for each subject. It was observed that AD patients showed a decrease of mean PLI in both the lower alpha and beta bands but not in the other bands. In the same lower alpha band, AD patients also exhibited decreased frontoparietal, frontotemporal, parieto-occipital, and temporo-occipital connectional strength (PLI), which was consistent with previous EEG/MEG AD studies (Jelic and others 1996; Stam and others 2006). Further graph theoretical analysis revealed that, in the lower alpha band, AD patients had lower normalized weighted clustering coefficients (C_w/C_w^{rand}) and path lengths (L_w/L_w^{rand}) as compared to controls. The organization of lower alpha band functional network in AD is in favor of a more random configuration. A significant correlation (Spearman $r = 0.475$, $P = 0.008$) was also detected between the MMSE score and normalized weighted clustering coefficients for all the subjects. By modeling the pathological process of AD using a simulation analysis, Stam and others (2009) further demonstrated that the AD-related network changes in the lower alpha could be better explained by a "Targeted Attack" model (assuming that edges connecting high-degree nodes are more vulnerable than others, causing their weight to be reduced first) instead of a "Random Failure" model (assuming that network changes are due to a random decrease in the strength of all edges). Their modeling analysis suggests that those highly connected brain network "hubs" (e.g., association cortex regions) might be especially at risk in AD. Although Stam and colleagues used different research approaches in the two studies (EEG vs. MEG, SL vs. PLI measurements, unweighted vs. weighted network analysis), they both demonstrated that AD patients were associated with disruptive system integrity in the large-scale functional brain networks as characterized by a weakening of small-world network characteristics.

fMRI

In contrast to EEG/MEG techniques, fMRI has relatively poor temporal resolution but decent spatial resolution. Conventionally, the AD-related studies of brain functional connectivity by fMRI focused on exploring abnormal functional interactions between brain regions of cognitive networks during a variety of tasks. For example, Bokde and others (2006) reported functional connectivity abnormalities in the fusiform gyrus during a face-matching task in subjects with mild cognitive
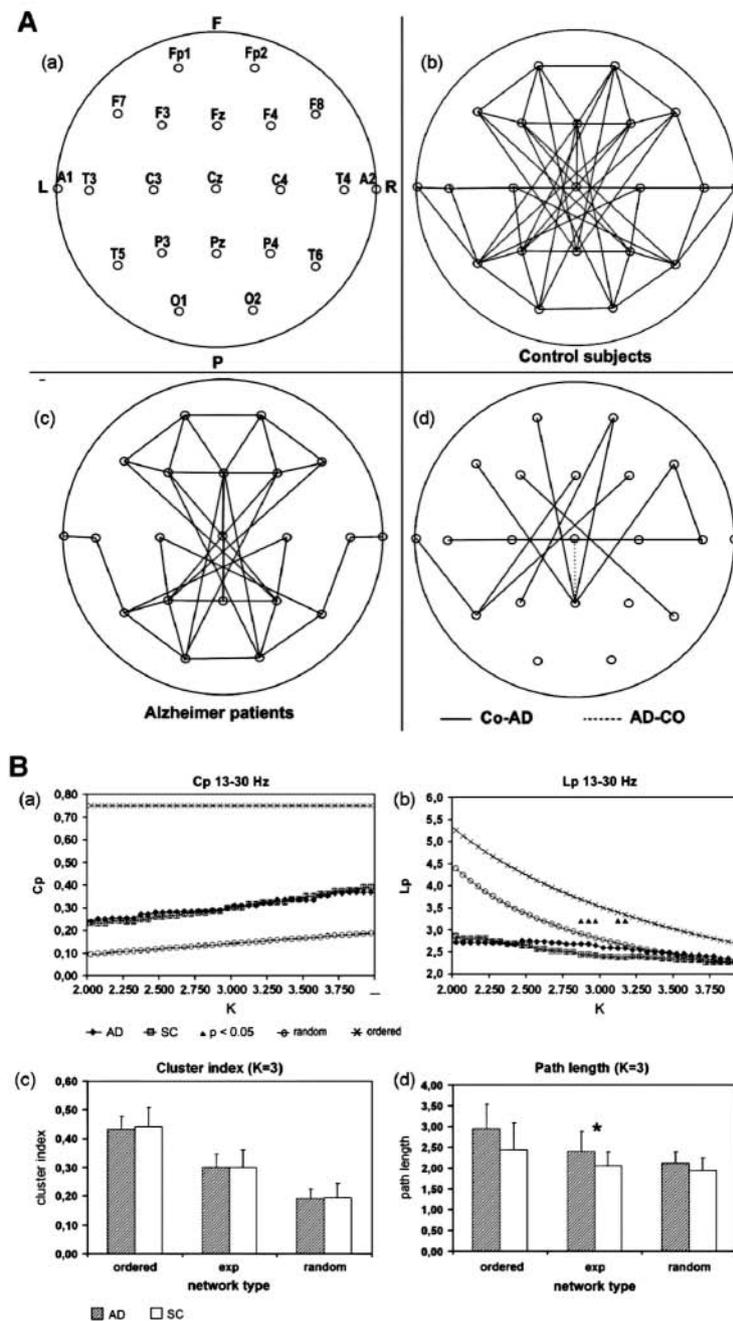
Figure 2. Construction of brain functional networks derived from electroencephalograph (EEG) data (*A*) and Alzheimer's disease (AD)–related changes in small-world network properties (*B*) (Stam and others 2007). (*A*) Brain functional networks constructed by calculating mean synchronization matrices of EEG data. (*a*) Schematic image of the head viewed from above, with the positions of the electrodes indicated by small circles and numbered according to the 10 to 20 electrode placement system. (*b*) Brain functional network of the control subjects. If the synchronization likelihood (SL) between two electrodes is above a threshold, the two nodes are connected by a line. (*c*) Brain functional network of the AD patients. (*d*) Differences between the two groups: Co-AD = edges only present in control group (solid lines), and AD-Co = edges only present in AD group (dotted line). F = frontal; P = posterior; L = left; R = right. (*B*) AD-related changes in the small-world network parameters. (*a*) Mean cluster coefficient *C* and (*b*) path length for the AD group (black diamonds) and the control group (open squares) as a function of node degree *K*. Error bars correspond to standard error of the mean. Black triangles indicate where the difference between the two groups is significant (*t*-test, $P < 0.05$). The theoretical values of *C* and *L* for ordered and random networks as a function of *K* are shown for comparison. (*a*) *C* increases as a function of *K*, but no significant differences found between the AD patients and control group are present. The cluster coefficient of the EEG data is intermediate between that of ordered and random networks. (*b*) For *K* between 2.850 and 3.15, the path length is significantly longer in the AD group. The path length of the EEG data *L* is much smaller than that of ordered networks and even smaller than that of random networks for *K* < 3.4. (*c*) Comparison of the experimental cluster coefficient and (*d*) path length with those of the constructed random and ordered matrices that preserve the degree sequences of their experimental counterparts. *C* is intermediate between that of ordered and random networks, whereas *L* of the EEG network is lower than that of ordered networks but approximately equal to that of random networks; also *L* of AD is significantly longer than that of controls (*).

Weighted graph analysis of MEG
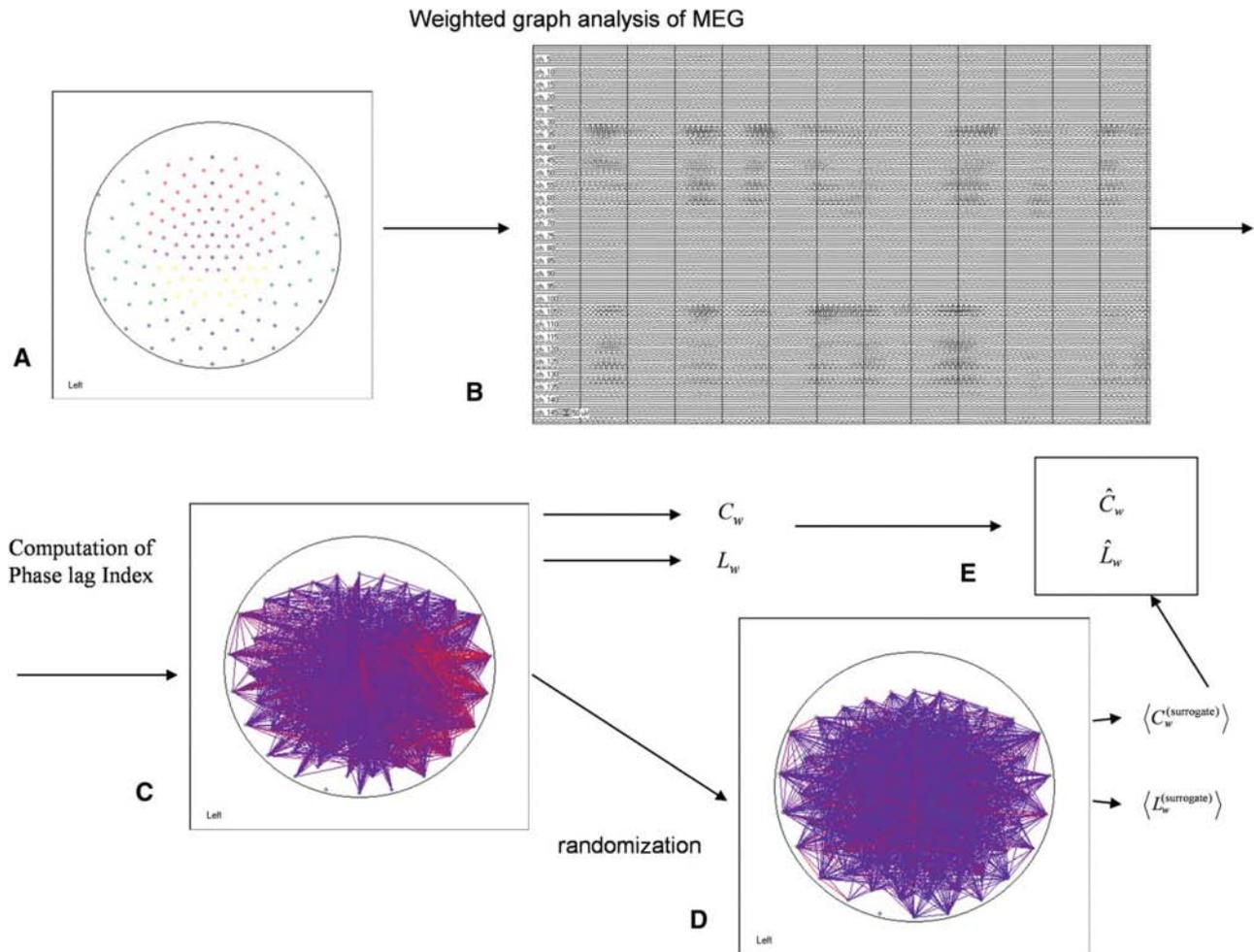
Figure 3.   Construction of brain functional networks derived from magnetoencephalograph (MEG) data (Stam and others 2009). Schematic illustration of the steps involved in weighted graph analysis of MEG recordings. At each of the MEG sensors, illustrated in (*A*), MEG signals are recorded. Epochs of MEG data are filtered, as shown in (*B*), and correlations between all pairs of channels are determined with the phase lag index (PLI). This resulted in a weighted graph, with the strength of the synchronization between pairs of sensors indicated in color (blue/red: low/high PLI), as shown in (*C*). From each graph, the weighted clustering coefficient C_w and the weighted path length L_w are computed. Also, from each graph, an ensemble of random graphs is generated by randomly shuffling the connection weights (*D*). The C_w and L_w of each of the random graphs are determined, and the mean values for the ensemble, $<C_w^{(surrogate)}>$ and $<L_w^{(surrogate)}>$, are determined. Finally, the ratios $C_w/<C_w^{(surrogate)}>$ and $L_w/<L_w^{(surrogate)}>$ are computed (*E*).

impairment (MCI) whose risk of conversion to AD is much higher than the cognitively normal subjects. Several other fMRI studies also reported that, during a simple motor task (Greicius and others 2004) and an associative memory task (Celone and others 2006), AD patients were associated with reduced functional interactions within a "default-mode" system (a memory-related neuronal network that is mainly comprised of the posterior cingulated cortex/precuneus, lateral temporal and parietal cortex, as well as the hippocampus and medial frontal cortex regions [Raichle and others 2001]). In addition to the task-state fMRI studies, resting-state functional connectivity was also analyzed in AD using fMRI. For instance, by investigating correlative

spontaneous activities among brain regions using resting fMRI, two recent studies demonstrated that AD patients had disrupted functional integrity between the hippocampus and many neocortical regions (Allen and others 2007; Wang and others 2006). In another resting fMRI study, Wang and others (2007) reported decreased functional connections between the prefrontal and parietal regions but increased connectivity within the prefrontal, parietal, and occipital lobes in AD patients. More recently, Sorg and colleagues (2007) found that MCI patients had reduced resting-state functional connectivity in both the executive attention system and default-mode network. These fMRI-based findings in AD networks are largely consistent with the

results from the EEG/MEG studies (Jelic and others 1996; Stam and others 2006) and other measures of the functional neuroimaging studies such as positron emission tomography (Grady and others 2001; Horwitz and others 1987). These studies suggest that AD patients are associated with loss of functional integrity within selective neuronal networks such as the hippocampal-based memory system, attention system, and default-mode network.

Similar to EEG/MEG approaches, fMRI has also been recently applied to investigate the global topological organization of large-scale brain functional networks in both the healthy subjects and AD patients. Salvador and colleagues (2005) were the first to utilize fMRI to investigate the functional connectivity patterns of the whole brain. They extracted average BOLD time series from 90 cortical and subcortical areas (45 from each hemisphere), acquired from 12 healthy volunteers in a resting state, and estimated inter-regional functional connectivity by calculating partial correlation coefficients between every pair of time series. After thresholding the mean group correlation matrix into a binary connectivity matrix, using graph theoretical analysis, they found that the brain functional network showed a small-world topology that was in accordance with previous functional data (EEG/MEG) analysis. Further multivariate statistical analysis using hierarchical clustering and multidimensional scaling demonstrated that the brain network included several major functional clusters corresponding to 4 neocortical lobes (frontal, temporal, parietal-(pre)motor, and occipital), medial temporal lobe, and subcortical nuclei. In a subsequent study from the same group, Achard and others (2006) applied the discrete wavelet transform to the resting fMRI time series obtained from five healthy volunteers and estimated frequency-dependent correlation matrices characterizing the functional connectivity among 90 brain regions. They found that the small-world topology of brain functional networks was most salient in the low-frequency interval of 0.03 to 0.06 Hz. Furthermore, they showed that the human brain functional network was dominated by a neocortical core of highly connected hubs that were mainly comprised of recently evolved brain regions of the heteromodal association cortex with long-distance connections to other regions. Similar topological properties have also been shown in several recent resting-state fMRI studies in healthy subjects (Achard and Bullmore 2007; Liu and others 2008; Wang, Wang, and others 2009; Wang, Zhu, and others 2009).

Using resting-state fMRI and graph theoretical network analysis, Supekar and colleagues (2008) demonstrated, for the first time, that AD patients were associated with disrupted small-world topological organization in the spontaneous brain functional networks (Table 1, Fig. 4). They collected resting fMRI data from 21 AD subjects and 18 age-matched controls and utilized wavelet analysis to acquire frequency-dependent correlation matrices among 90 brain regions. After thresholding the correlation matrices into a set of undirected brain functional networks, they compared small-world parameters between the AD patients and normal controls and found that AD patients showed deteriorations of the small-world network properties, characterized by a significantly lower normalized clustering coefficient, C_p/C_p^{rand} ($P < 0.01$), implying a disrupted local network connectivity. Furthermore, the differences in the normalized clustering coefficient can be applied to distinguish the AD participants from the controls with a sensitivity of 72% and a specificity of 78%, suggesting that these network measures may be useful as an imaging-based biomarker in AD diagnosis. In their study, they also found that clustering coefficients of the bilateral hippocampus were significantly lower ($P < 0.01$) in the AD group compared to the control group. These findings suggest that AD patients are associated with disrupted functional integrity in the intrinsic spontaneous neuronal activity of the brain functional system.

In summary, human neurophysiological and functional neuroimaging data have provided strong evidence of abnormal functional integrity in the large-scale neuronal communication networks in AD, which is likely to be part of explanations in the declines of mnemonic and other cognitive functions in AD.

Structural Brain Networks in AD

Most imaging studies of brain connectivity in AD have been mainly focused upon exploring the abnormalities of functional connectivity patterns as described previously. The network of structural connectivity has been less studied in both the healthy populations and AD patients because the common invasive tracing methods used in the analysis of mammalian structural brain networks such as the cat and primate cannot be directly applied to the human brain (Crick and Jones 1993). In this section, we will review recent progress made in analyzing the structural and diffusion MR images that allow us to noninvasively map abnormal structural connectivity patterns in AD.

Structural MRI

Over the past two decades, structural MRI (sMRI) has been widely used to study gray matter morphology (e.g., volume, density, and thickness) of the human cortex. The ubiquitous brain morphometric data have been nevertheless largely overlooked in most brain network analyses. Recently, many researchers have demonstrated that the morphological features of the human cerebral
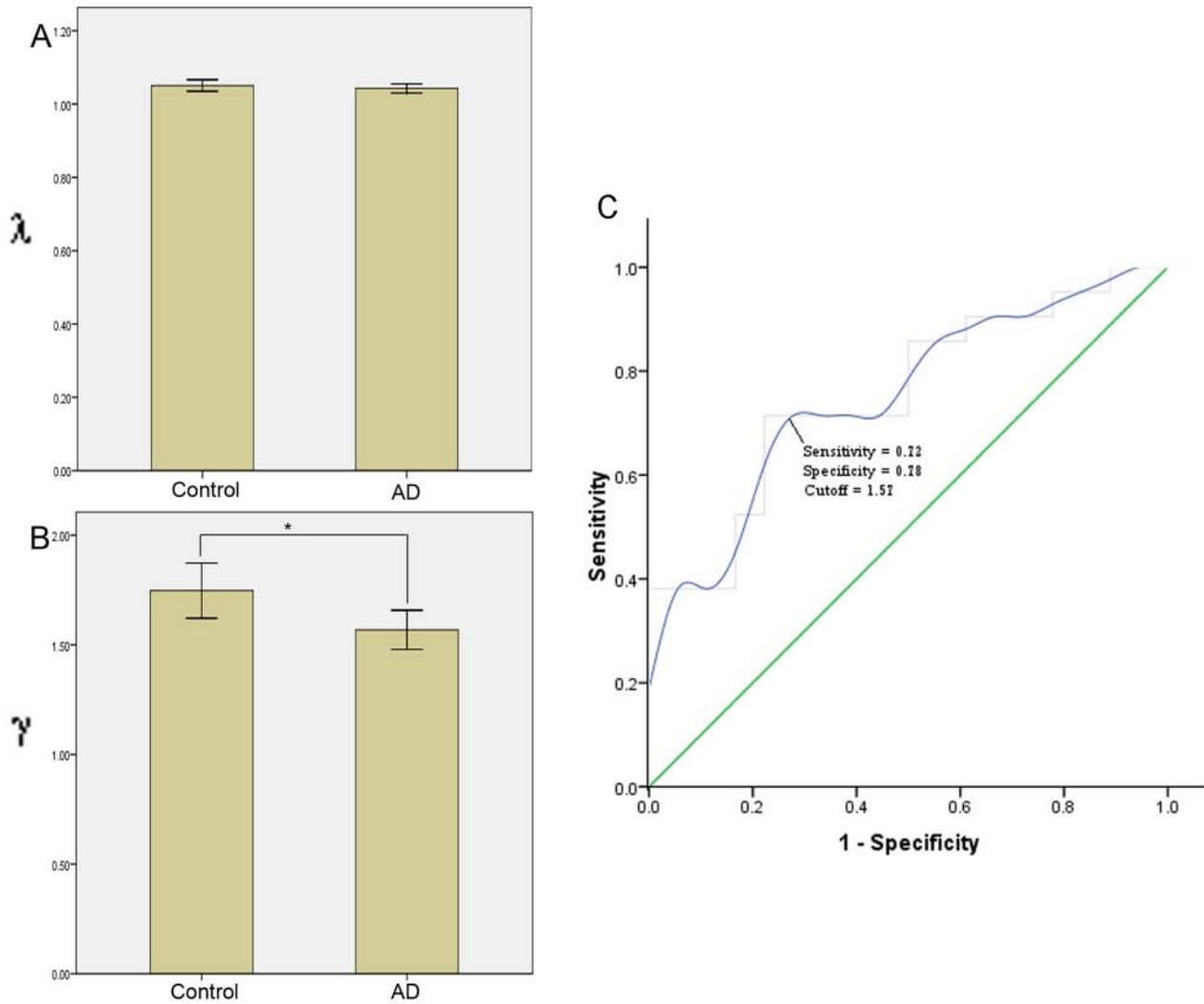
Figure 4. Alzheimer's disease (AD)–related changes in small-world properties of brain functional networks derived from resting functional magnetic resonance imaging (fMRI) data (Supekar and others 2008). (A) Mean clustering coefficient, λ (L/L_{ran}), values for the AD group and the control group. No significant differences in the mean λ values are observed. (B) Mean characteristic path length, γ (C/C_{ran}), values for the AD group and the control group. The γ values in AD group were significantly lower (indicated by *) than that in the control group ($P < 0.01$). (C) Receiver operating characteristic curve, plot of the sensitivity (1-specificity), for distinguishing AD participants from controls as a function of varying normalized clustering coefficient (γ) threshold. Using a cut-off value of 1.57, γ correctly classified 14 of 18 controls and 15 of 21 AD subjects, yielding 72% sensitivity and 78% specificity. The area under the curve was 0.754 (95% confidence interval [CI] area, 0.602–0.906).

cortex derived from sMRI carry important brain connectivity information. For instance, several researchers have observed strong correlations in gray matter morphological features between various anatomically or functionally linked areas of the human brain such as the frontotemporal (Bullmore and others 1998; Lerch and others 2006), frontoparietal (Wright and others 1999), contralateral interhemispheric (Mechelli and others 2005), and visual-associated regions (Andrews and others 1997). These structural correlations might be a result of the mutually trophic influences (Ferrer and others 1995), the contribution of heredity (Thompson and others 2001), or common experience-related plasticity (Maguire and others 2000).

Recently, He, Chen, and Evans (2007) developed a systematic methodology, GRETNA (Fig. 2), for characterizing the patterns of structural correlation (morphological connectivity) across the entire human cerebral cortex. They first extracted the regional cortical thickness using advanced computational techniques (Kim and others 2005; MacDonald and others 2000) and then calculated inter-regional thickness associations, followed by a graph theoretical analysis. When GRETNA was applied to the brain sMRI data from 124 right-handed normal adults, a cortical network composed of 45 brain regions (27 for each hemisphere) and 102 connections was generated (~7% of all possible connections). In the structural brain

network, many of the connections had approximate correspondence to those known functional or anatomical connections of the human brain. Furthermore, GRETNA revealed many important statistical properties underlying the organization of the human cortical structural network, including the small-worldness (i.e., high local clustering and short paths), truncated power-law degree distribution, and various network hub regions that were mainly related to the association cortex (He, Chen, and Evans 2007). Recently, GRETNA was also applied to reveal the modular architecture of the normal structural brain network that corresponds to six known brain functional neuroanatomy modules (Chen and others 2008). Each module was characterized by its denser intramodule connections (Newman and Girvan 2004). The segregation of the six modules with apparent functional significance suggests that functional organization of human brain networks may have a highly modularized structural correlate. Many of these results are consistent with previous human functional brain network studies (Achard and others 2006; Salvador and others 2005). Interestingly, two recent studies (Bassett and others 2008; He, Chen, Rosa, and others 2007) have used other brain morphological features such as gray matter volume to construct brain structural networks in healthy subjects and also demonstrated similar network topological properties as previously shown in the human cortical thickness networks. These sMRI studies provided strong evidence supporting that the morphology of the human cerebral cortex has evolved into an optimal neural architecture to support both modularized and distributed information processing by maximizing the efficiency of information propagation and minimizing wiring costs (Achard and Bullmore 2007; Bassett and Bullmore 2006; Kaiser and Hilgetag 2006; Sporns and others 2004).

Structural MRI has also received considerable attention as a promising in vivo technique in characterizing brain disease pathology and progression. In AD studies, different structural properties evaluated using various voxel/vertex-based morphometrics have revealed the loss of gray matter in the hippocampal and entorhinal cortices that are vital nodal regions in the memory networks, and they further provide surrogate biomarkers for many therapeutic trials (for a review, see Apostolova and Thompson 2008). Some researchers have also observed that the structural changes in the AD patient's brain appear to be in a widespread fashion but are mainly located at some selective brain areas such as the temporal and limbic cortices (Lerch and others 2005; Singh and others 2006; Thompson and others 2003). Specifically, in a longitudinal MRI AD study, Buckner and colleagues (2005) demonstrated that the early-stage AD patients had prominent regional atrophy in the components of the "default" system

(posterior cingulate cortex, hippocampus, retrosplenial and lateral parietal cortex) that are thought to be mainly involved in episodic memory processing, suggesting a preferential affection of this disease on the neuronal network. The similar pattern of regional cortical atrophy in early AD has also been shown by using cortical mapping approaches (Lerch and others 2005; Singh and others 2006). Despite a lack of structural brain connectivity analysis in previous studies, these results suggest that the gray matter loss in AD might be in a manner of correlative changes in some specific regions of the neuronal networks.

He and colleagues were the first to use MR-based morphometric features to compare the patterns of structural connectivity between AD patients and healthy controls (He, Chen, and Evans 2008) (Table 1). They constructed regional cortical thickness correlation matrices for both groups (92 early-stage AD subjects and 97 normal controls) (Fig. 5) and found many significant alterations in the connection strength between brain regions in AD. One observation was the disruption of the structural correlations between the bilateral parietal regions in AD patients, which is in accordance with many electrophysiological and neuroimaging studies in AD. Additionally, they also observed that AD patients showed regional cortical thinning and increased inter-regional thickness correlations in the "default-mode" network (including the lateral temporal and parietal cortex, as well as the cingulate and medial frontal cortex regions) that has been known to exhibit AD-related breakdown of brain activities, such as amyloid deposition and metabolic and spontaneous activity disruption (Buckner and others 2005; Celone and others 2006; Dosenbach and others 2007; Greicius and others 2004; Wang and others 2006). The abnormality of structural correlations may be attributed to the AD-related ultrastructural changes such as the local cell death/shrinkage, reduced dendritic extent, and synaptic loss, although the underlying neurobiological basis remains to be further elucidated.

In addition to the inter-regional cortical thickness correlation analysis, more importantly, He and colleagues also performed a network analysis (GRETNA) on both the AD and normal groups. They found that, although both groups exhibited small-world topology in their structural cortical networks, the AD patients demonstrated larger clustering coefficients, C_p, and longer shortest path length, L_p, suggesting a less optimal network topological organization (Fig. 6). Short paths in brain networks assure effective integrity or rapid transfers of information between and across remote regions that are believed to constitute the basis of cognitive processes (Sporns and others 2004); therefore, the AD-related increases in path length might reflect disrupted neuronal integrations among distant brain regions. This result was in accordance with previous
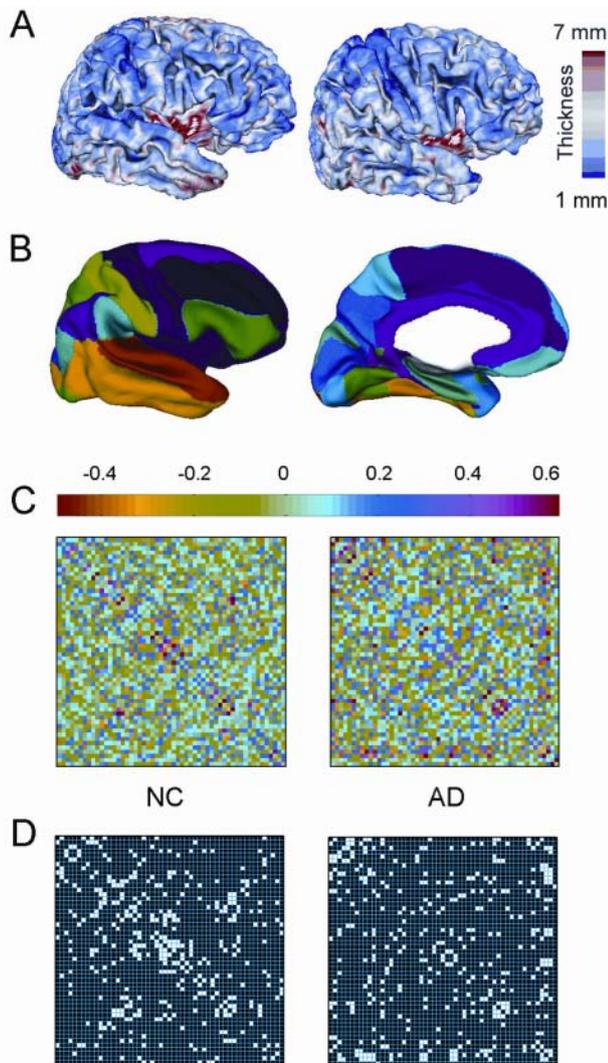
Figure 5. Construction of structural cortical networks derived from structural magnetic resonance imaging (sMRI) data (He, Chen, and Evans 2008). (*A*) Two representative cortical thickness maps (*left* for a control subject and *right* for an Alzheimer's disease [AD] subject) were obtained from anatomical MRI by computational neuroanatomy. The color bar indicates the range of cortical thickness shown on the *right*. (*B*) The entire cerebral cortex was segmented into 54 cortical areas that were displayed on the average cortex (*left* for the lateral surface and *right* for the medial surface), with each color representing a defined brain region. (*C*) The correlation matrices were obtained by calculating partial correlations between regional thickness across subjects within each group (*left* for the control group and *right* for the AD group). The color bar indicating the partial correlation coefficient between regional cortical thickness is shown on the *top*. (*D*) The correlation matrices of *C* were thresholded into the binarized matrices (*left* for the control group and *right* for the AD group) by a sparsity threshold of 13%. Such a threshold ensures that the networks of both of the groups have the same number of nodes and links (i.e., the two networks have the same wiring cost). NC = normal controls.

brain functional network analysis using EEG (Stam and others 2007). In the study, He and others also investigated AD-related changes in the nodal characteristics of the structural brain networks (Fig. 6). The AD patients

were found to show significantly decreased nodal centrality in several heteromodal association cortex regions (e.g., superior temporal gyrus and angular gyrus) that have rich long-range anatomical connections with many other cortical regions. These regions tend to have a higher topological centrality in the healthy brain networks. Thus, the abnormalities of nodal centrality in AD may reflect a disruptive integration of large-scale brain networks. Increases in the nodal centrality were also found in several unimodal association cortex regions (e.g., lingual gyrus and lateral occipitotemporal gyrus) that usually retain their functional capacity in early AD (Grady and others 1988; Mentis and others 1996). The increases in those regional centrality are consistent with previous findings of increased regional activation (Backman and others 2000; Dosenbach and others 2007; He, Wang, and others 2007; Prvulovic and others 2002) and functional connectivity (Grady and others 2003; Horwitz and others 1995) that were characterized as compensatory recruitment of cognitive resources to maintain task performance in AD.

This study by He and colleagues also examined the topological robustness of the structural brain networks in response to random failures and targeted attacks (Albert and others 2000) (Fig. 7). In healthy subjects, the structural brain network exhibits high resilience when its nodes and links are attacked in both manners (Achard and others 2006; Kaiser and Hilgetag 2004). In AD patients, He and others found that the structural brain network was extremely vulnerable to targeted attacks on its pivotal nodes and links in comparison to the controls, presumably a reflection of abnormal topological organization in AD, such as the aberrant structural correlations, small-world architecture, and nodal centrality.

As for the morphometry-based brain network analysis, it should be kept in mind that the brain networks were constructed by calculating the correlations of regional morphological correlations across a group of subjects. Thus, one could not establish a single structural brain network in an individual subject. Nonetheless, we have recently demonstrated that the overall small-world network efficiency in patients with multiple sclerosis was significantly disrupted in a manner proportional to the extent of total white matter lesions by classifying a large sample of 330 patients into 6 subgroups according to their lesion loads (He, Dagher, and others 2009). Thus, one may expect to see a decline in AD network efficiency with increasing disease. The idea is to bring out the generalizability of the GRETNA method and to demonstrate how it could be used as a biomarker of disease progression in AD.

Diffusion MRI

In addition to sMRI, the patterns of structural connectivity of the human brain in vivo can also be studied
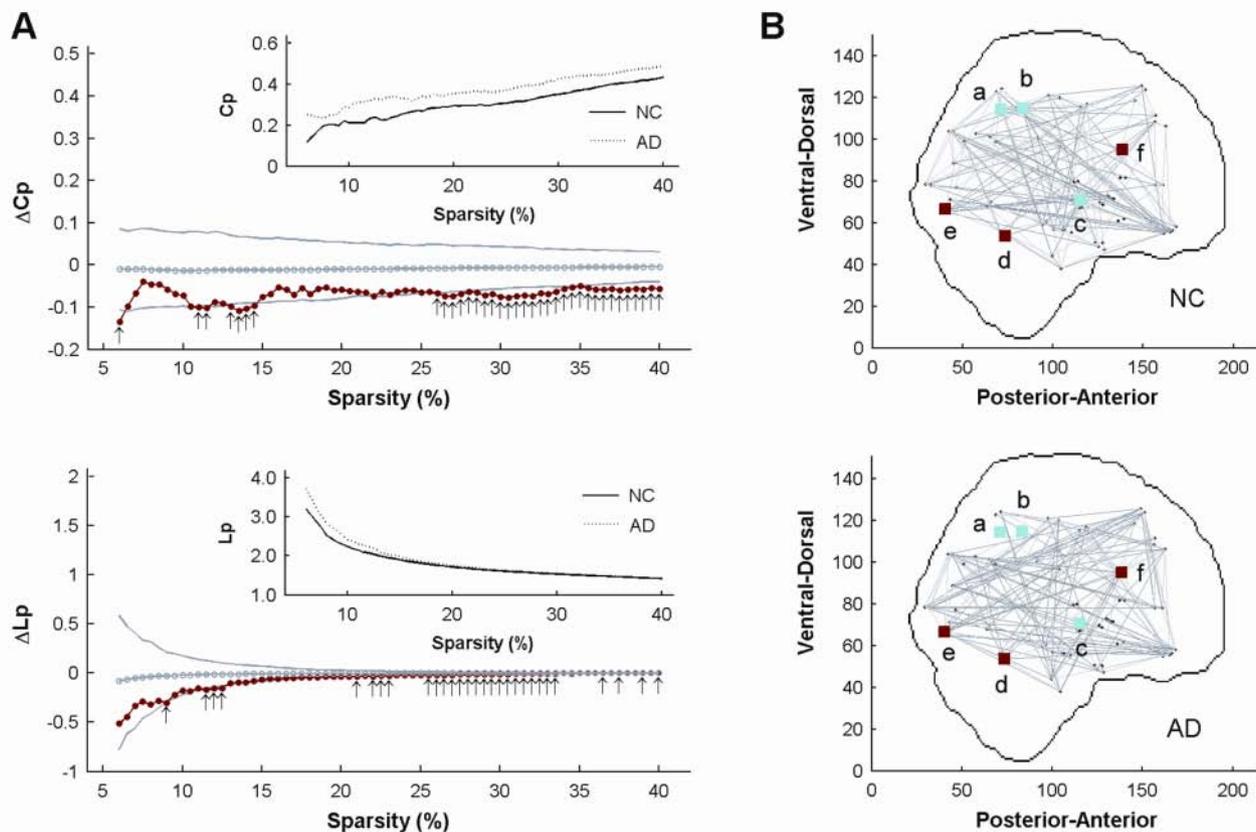
Figure 6. Alzheimer's disease (AD)–related changes in small-world properties of structural cortical networks (He, Chen, and Evans 2008). (*A*) Between-group differences in clustering coefficient (C_p) and path length (L_p) as a function of sparsity. The *upper* graph shows the differences (red circles) in the C_p between the controls and AD patients as a function of sparsity thresholds. The gray lines represent the mean values (open circles) and 95% confidence intervals of the between-group differences obtained from 1000 permutation tests at each sparsity value. Arrows indicate a significant ($P < 0.05$) difference in C_p between the two groups. Note that AD patients (dotted lines) show larger C_p values in the brain networks than controls (solid lines) over a wide range of thresholds (inserted panel). The *lower* graph shows the differences (red circles) in the L_p between the controls and AD patients as a function of sparsity thresholds. The gray lines represent the mean values (open circles) and 95% confidence intervals of the between-group differences obtained from 1000 permutation tests at each sparsity value. Arrows indicate a significant ($P < 0.05$) difference in L_p between the two groups. Note that AD patients (dotted lines) show larger L_p values in the brain networks than controls (solid lines) over a wide range of thresholds (inserted panel). (*B*) Regions showing significant AD-related changes in b_i were mapped to anatomical space in the control (*upper* panel) and AD (*lower* panel) groups. Regions showing AD-related decreases are colored in cyan, and regions showing AD-related increases are colored in red. Black lines represent the links of the networks. Note that these results were obtained from the brain networks with a sparsity of 13%. NC = normal controls.

with a diffusion MRI-based tractography method (also called fiber tracking). Diffusion MRI is capable of characterizing the orientation of white matter fiber bundles by detecting the underlying water molecule diffusion (for a review, see Le Bihan 2003). Using the fiber orientation information of each brain voxel, deterministic "streamline" tractography based upon diffusion tensor imaging (DTI) was widely used to infer the continuity of fiber bundles from one voxel to the other (Mori and van Zijl 2002). With multiple manual/automatic regions of interest (ROIs) selection, this deterministic tractography can yield major white matter tracts faithful to the known white matter anatomy (Catani and others 2002; Wakana and others 2004). Recently, probabilistic tractography approaches that focus on the connectivity

probabilities rather than the actual white matter pathways between voxels have been proposed and applied more and more widely (Behrens and others 2003; Parker and Alexander 2005). To date, the diffusion MRI tractography methods provide a unique tool to infer the anatomical connectivity between any brain voxels or regions in vivo.

In AD-related diffusion MRI studies, the abnormalities of brain structural connectivity (i.e., white matter integrity) have also been reported. For instance, many investigators have shown significant reduction in the integrity of the major white matter tracts such as the splenium of the corpus callosum (Bozzali and others 2002; Rose and others 2000; Stahl and others 2003; Ukmar and others 2008), superior longitudinal
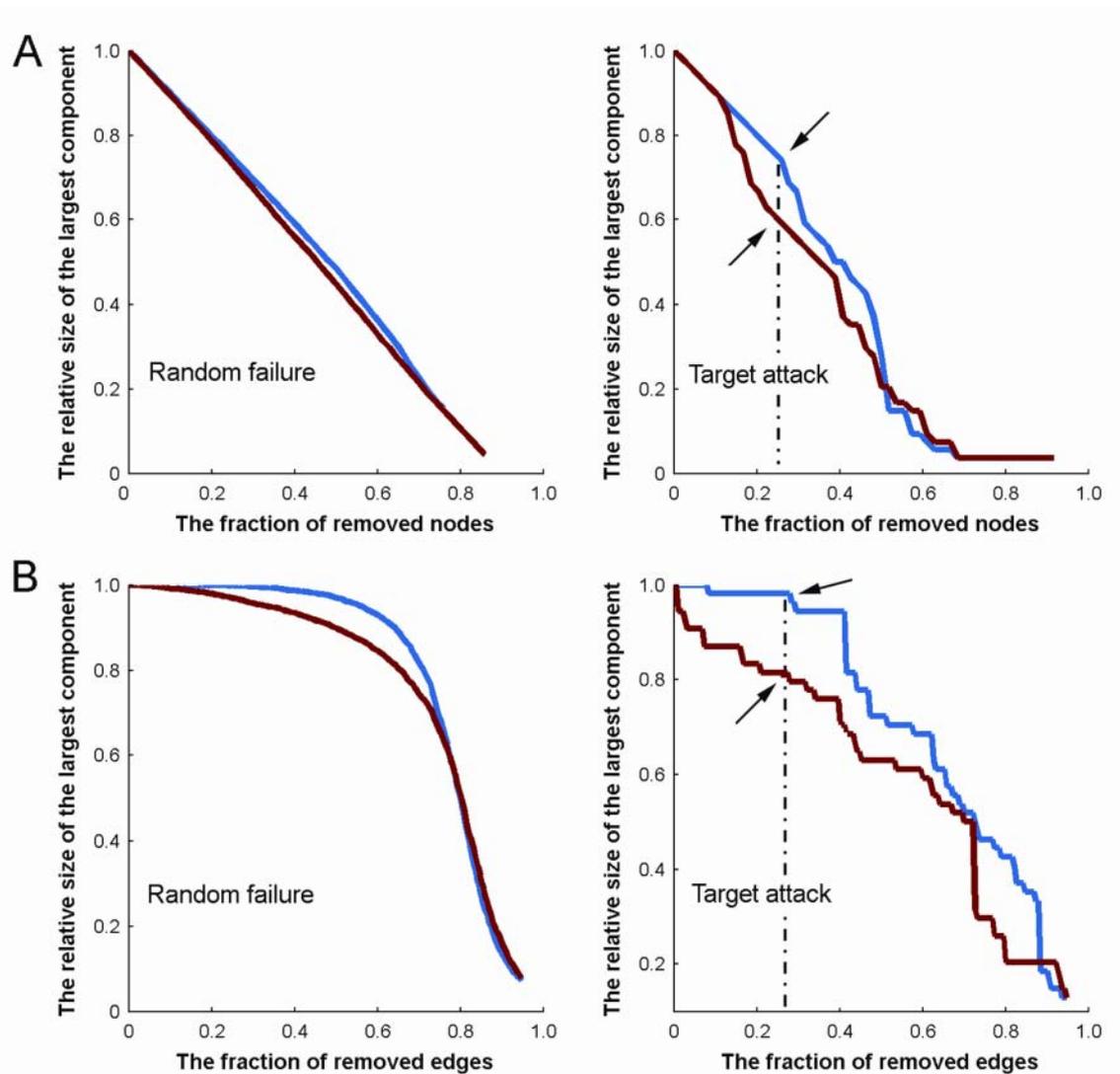
Figure 7. Alzheimer's disease (AD)–related changes in topological robustness in structural cortical networks (He, Chen, and Evans 2008). The graphs show the relative size of the largest connected component as a function of the fraction of removed nodes (*A*) and links (*B*) by random failures (*left* panel) or targeted attacks (*right* panel). The brain network in the AD patients (red line) was approximately as robust as that in the controls (blue line) in response to random failures. However, it displayed remarkably reduced stability against targeted attack compared with the control network. Note that both brain networks used here had a same sparsity value of 13%. NC = normal controls.

fasciculus (Rose and others 2000; Xie and others 2006), cingulate bundles (Fellgiebel and others 2008; Rose and others 2000), and inferior fronto-occipital fasciculus (Fellgiebel and others 2008), as well as degeneration of nondominant white matter tracts in the frontal, temporal, and parietal lobes (Bozzali and others 2002; Ukmar and others 2008; Xie and others 2006). These impairments of local axonal integrity may result in the disruption of short- and/or long-range anatomical connectivity, which provides direct evidence for structural abnormalities in the neuronal networks of AD.

Recently, the diffusion MRI-based tractography methods have also been used to study the topological organization of large-scale human brain structural networks. Using diffusion spectrum imaging combined with the streamline tractography, Hagmann and colleagues (2007) demonstrated, for the first time, the small-world topology in the structural brain networks in two healthy human subjects. This study defined network nodes subject-specifically at a voxel population level (i.e., thousands of small ROIs). The uncovered small worldness in the human structural networks indicates that the neuronal pathways of the human brain are structurally organized into an optimal architecture characterized by a segregated and integrative connectivity mode. In a subsequent study, Hagmann and others (2008) further used diffusion spectrum imaging to investigate the modular and core structure of the human cerebral cortical networks in five healthy subjects and found that those network hubs linking different

structural modules are mainly located at the posterior-medial-parietal cortices. Another study, done by Iturria-Medina and others (2008), constructed a weighted human structural brain network at a regional level for each individual brain using diffusion MRI-based "anatomical connection probabilities" in a group of 20 normal subjects and further demonstrated a broad range of the common network characteristics, such as small worldness and efficiency. More recently, Gong and others (2009) proposed a population-based anatomical network framework also at a regional level, however, using diffusion tensor imaging streamline tractography. The constructed cortical network captured the underlying backbone connectivity pattern of the human cerebral cortex across a large population ($n = 80$) of healthy young adults and demonstrated compatible network characteristics (e.g., small worldness) that were in accordance with previous studies. Notably, the medial-parietal cortices (e.g., precuneus) that form the posterior components of the human default network were consistently identified as the most central regions in the human brain structural networks in both the studies of Gong and others (2009) and Hagmann and others (2008).

To date, however, no studies have used diffusion MRI techniques to examine AD-related alterations in the topological organization of the whole-brain structural networks. Based on previous observations that AD patients show not only diffuse abnormalities in many white matter bundles but also aberrant connectivity patterns in large-scale functional (Stam and others 2009; Stam and others 2007; Supekar and others 2008) and structural (morphological) (He, Chen, and Evans 2008) brain networks, one could speculate that AD patients are more likely to have aberrant topological organization (e.g., small-world parameters and nodal centrality) in the anatomical brain networks based upon white matter bundles. These studies would be crucial for our further understanding of how brain structural abnormalities in patients with AD underlie their functional disruption. However, one should be cautious when applying the diffusion MRI tractography-based techniques to study the structural brain networks. The tractography algorithms are prone to spurious connections (i.e., false positive) due to the image noises or algorithm limitations (Parker and Alexander 2005). On the other hand, it is well recognized that current tractography methods using diffusion MRI remain powerless in the regions of fiber crossing, likely leading to the loss of true fiber bundle connections (i.e., false negative) in the anatomical brain networks (Gong and others 2009). For example, fiber bundles that are involved in interhemispheric connections of lateral cortical regions are frequently missed by current tractography methods.

In summary, the noninvasive structural and diffusion MRI techniques have provided a promising experimental route toward revealing human brain structural

connectivity patterns in vivo in both the healthy subjects and AD patients. The study of structural connectivity networks in AD has important implications on our understanding of how brain structural abnormalities in patients underlie functional deficits of the brain.

Future Perspectives

Recent literature examined in this review has strongly suggested that AD patients are associated with disrupted functional and structural integrity in multiple distributed neuronal networks as well as in the whole-brain system, which brings promises to revolutionize our views of the underlying disease mechanism in AD. However, we should acknowledge that the studies of complex brain networks in AD, even in normal subjects, are at their infant stages. There are still a number of unanswered questions in this research field.

Firstly, how are the abnormalities in the large-scale (i.e., regional level) brain networks observed in these studies correlated to the damages at smaller organization levels, such as neurons and local populations of neurons (e.g., cortical minicolumns)? Computational simulations and empirical studies on these basic neuronal elements and their connectivity patterns would be helpful to address this issue (Sporns and others 2005).

Secondly, what are the relations among the abnormalities of functional, morphological, and structural brain networks in AD? Given the fact that most of the studies in AD so far were separately conducted using structural and functional data, it is not clear how the changes of brain structural connectivity correlate to that of functional connectivity. The quality and scope of the available data hinder our ability to perform a more comprehensive structural-functional network analysis. There are currently very few publicly available data sets including multimodality images (e.g., fMRI, sMRI, and DTI) in both the healthy human subjects and AD patients, but they would be extremely crucial for us to facilitate different information integration about the normal or pathological status of the same neuronal system. Such an analysis would offer a unique insight into the understanding of the structural basis underlying the brain functional states and how the structural connectivity disruption in AD reflects functional deficits.

Thirdly, few articles discussed in this review focused on the topological changes in the large-scale neuronal networks during the performance of tasks. In fact, many previous studies have suggested that AD patients would show the impairments of memory and other cognitive functions that are accompanied by regional alterations in the functional activation. However, it would be desirable to perform a more extensive reanalysis of these previously published AD data that are

likely able to offer new insights for mechanistic modeling and reinterpretation of the results.

Fourthly, the literature reviewed here strongly suggested that both AD and MCI (a higher risk for converting to AD) patients had abnormal neuronal integrity; however, it is unknown how the topological organization of brain networks alters at the conversion stage as disease progresses. Longitudinal studies will be helpful to clarify this issue. In addition, it would also be interesting to look at whether the carriers of the APOE-4 gene (a genetic risk factor for AD) show similar changes in their neuronal networks as previously demonstrated in AD.

Fifthly, most of the studies have demonstrated the abnormal brain connectivity in AD patients. It remains to be elucidated about whether these findings are only specific to AD or might also be observed in other types of dementia such as vascular dementia and dementia with Lewy bodies. In other words, can the changes in the topological parameters of the AD brain networks serve as valid biological markers for the disease diagnosis?

Finally, most current brain network computational methods have overlooked a lot of important information of the brain structures. For example, the dynamic relationship between different brain regions is usually neglected in the present brain functional network analysis; however, it is crucial to be able to capture a time-varying topological structure in the brain system. In addition, the construction and analysis of complex brain networks also need to be further improved in the future, which includes a comprehensive analysis about the network node definition on the basis of functional activation and different brain atlases, a more detailed description of network edges according to specific functional and structural connectivity information, and the analysis of different types of brain networks such as the binary versus weighted networks and undirected versus directed networks.

Conclusion

Taken together, converging evidence from these multiple lines of studies suggests that AD patients had disruptive system integrity in their neuronal networks that could be responsible for cognitive and memory declines, thus potentially opening up a new window into our understanding of basic mechanisms of this disease. These topology-based network methods might also offer a novel route to diagnose and monitor the progression of AD in clinics. Future studies in AD such as those using multimodal neuroimaging techniques, theoretical modeling, and modern graph theoretical network analysis could be conducted to further uncover the underlying biological basis of this disease.

References

Achard S, Bullmore E. 2007. Efficiency and cost of economical brain functional networks. PLoS Comput Biol 3(2):e17.

Achard S, Salvador R, Whitcher B, Suckling J, Bullmore E. 2006. A resilient, low-frequency, small-world human brain functional network with highly connected association cortical hubs. J Neurosci 26(1):63–72.

Adler G, Brassen S, Jajcevic A. 2003. EEG coherence in Alzheimer's dementia. J Neural Transm 110(9):1051–8.

Albert R, Jeong H, Barabasi AL. 2000. Error and attack tolerance of complex networks. Nature 406(6794):378–82.

Allen G, Barnard H, McColl R, Hester AL, Fields JA, Weiner MF, and others. 2007. Reduced hippocampal functional connectivity in Alzheimer disease. Arch Neurol 64(10):1482–7.

Andrews TJ, Halpern SD, Purves D. 1997. Correlated size variations in human visual cortex, lateral geniculate nucleus, and optic tract. J Neurosci 17(8):2859–68.

Apostolova LG, Thompson PM. 2008. Mapping progressive brain structural changes in early Alzheimer's disease and mild cognitive impairment. Neuropsychologia 46(6):1597–612.

Backman L, Almkvist O, Nyberg L, Andersson J. 2000. Functional changes in brain activity during priming in Alzheimer's disease. J Cogn Neurosci 12(1):134–41.

Bang-Jensen J, Gutin G. 2000. Digraphs: Theory, Algorithms and Applications. Springer-Verlag, London.

Bassett DS, Bullmore E. 2006. Small-world brain networks. Neuroscientist 12(6):512–23.

Bassett DS, Bullmore E, Verchinski BA, Mattay VS, Weinberger DR, Meyer-Lindenberg A. 2008. Hierarchical organization of human cortical networks in health and schizophrenia. J Neurosci 28(37):9239–48.

Bassett DS, Meyer-Lindenberg A, Achard S, Duke T, Bullmore E. 2006. Adaptive reconfiguration of fractal small-world human brain functional networks. Proc Natl Acad Sci U S A 103(51):19518–23.

Behrens TE, Woolrich MW, Jenkinson M, Johansen-Berg H, Nunes RG, Clare S, and others. 2003. Characterization and propagation of uncertainty in diffusion-weighted MR imaging. Magn Reson Med 50(5):1077–88.

Berendse HW, Verbunt JP, Scheltens P, van Dijk BW, Jonkman EJ. 2000. Magnetoencephalographic analysis of cortical activity in Alzheimer's disease: a pilot study. Clin Neurophysiol 111(4):604–12.

Besthorn C, Forstl H, Geiger-Kabisch C, Sattel H, Gasser T, Schreiter-Gasser U. 1994. EEG coherence in Alzheimer disease. Electroencephalogr Clin Neurophysiol 90(3):242–5.

Boccaletti S, Latora V, Moreno Y, Chavez M, Hwang D. 2006. Complex networks: structure and dynamics. Phys Reports (424):175–308.

Bokde AL, Lopez-Bayo P, Meindl T, Pechler S, Born C, Faltraco F, and others. 2006. Functional connectivity of the fusiform gyrus during a face-matching task in subjects with mild cognitive impairment. Brain 129(Pt 5):1113–24.

Bozzali M, Falini A, Franceschi M, Cercignani M, Zuffi M, Scotti G, and others. 2002. White matter damage in

Alzheimer's disease assessed in vivo using diffusion tensor magnetic resonance imaging. J Neurol Neurosurg Psychiatry 72(6):742–6.

Buckner RL, Snyder AZ, Shannon BJ, LaRossa G, Sachs R, Fotenos AF, and others. 2005. Molecular, structural, and functional characterization of Alzheimer's disease: evidence for a relationship between default activity, amyloid, and memory. J Neurosci 25(34):7709–17.

Bullmore ET, Woodruff PW, Wright IC, Rabe-Hesketh S, Howard RJ, Shuriquie N, and others. 1998. Does dysplasia cause anatomical dysconnectivity in schizophrenia? Schizophr Res 30(2):127–35.

Catani M, Howard RJ, Pajevic S, Jones DK. 2002. Virtual in vivo interactive dissection of white matter fasciculi in the human brain. Neuroimage 17(1):77–94.

Celone KA, Calhoun VD, Dickerson BC, Atri A, Chua EF, Miller SL, and others. 2006. Alterations in memory networks in mild cognitive impairment and Alzheimer's disease: an independent component analysis. J Neurosci 26(40):10222–31.

Chen ZJ, He Y, Rosa-Neto P, Germann J, Evans AC. 2008. Revealing modular architecture of human brain structural networks by using cortical thickness from MRI. Cereb Cortex 18(10):2374–81.

Crick F, Jones E. 1993. Backwardness of human neuroanatomy. Nature 361(6408):109–10.

Delbeuck X, Van der Linden M, Collette F. 2003. Alzheimer's disease as a disconnection syndrome? Neuropsychol Rev 13(2):79–92.

Dickerson BC, Sperling RA. 2005. Neuroimaging biomarkers for clinical trials of disease-modifying therapies in Alzheimer's disease. NeuroRx 2(2):348–60.

Dosenbach NU, Fair DA, Miezin FM, Cohen AL, Wenger KK, Dosenbach RA, and others. 2007. Distinct brain networks for adaptive and stable task control in humans. Proc Natl Acad Sci U S A 104(26):11073–8.

Fellgiebel A, Schermuly I, Gerhard A, Keller I, Albrecht J, Weibrich C, and others. 2008. Functional relevant loss of long association fibre tracts integrity in early Alzheimer's disease. Neuropsychologia 46(6):1698–706.

Ferrer I, Blanco R, Carulla M, Condom M, Alcantara S, Olive M, and others. 1995. Transforming growth factor-alpha immunoreactivity in the developing and adult brain. Neuroscience 66(1):189–99.

Ferri R, Rundo F, Bruni O, Terzano MG, Stam CJ. 2007. Small-world network organization of functional connectivity of EEG slow-wave activity during sleep. Clin Neurophysiol 118(2):449–56.

Freeman LC. 1977. A set of measures of centrality based upon betweenness. Sociometry 40:35–41.

Friston KJ, Frith CD, Frackowiak RSJ. 1993. Time-dependent changes in effective connectivity measured with PET. Hum Brain Mapp 1:69–80.

Friston KJ, Frith CD, Liddle PF, Frackowiak RS. 1993. Functional connectivity: the principal-component analysis of large (PET) data sets. J Cereb Blood Flow Metab 13(1):5–14.

Gong G, He Y, Concha L, Lebel C, Gross DW, Evans AC, and others. 2009. Mapping anatomical connectivity patterns of human cerebral cortex using in vivo diffusion tensor imaging tractography. Cereb Cortex 19(3):524–36.

Grady CL, Furey ML, Pietrini P, Horwitz B, Rapoport SI. 2001. Altered brain functional connectivity and impaired short-term memory in Alzheimer's disease. Brain 124(Pt 4):739–56.

Grady CL, Haxby JV, Horwitz B, Sundaram M, Berg G, Schapiro M, and others. 1988. Longitudinal study of the early neuropsychological and cerebral metabolic changes in dementia of the Alzheimer type. J Clin Exp Neuropsychol 10(5):576–96.

Grady CL, McIntosh AR, Beig S, Keightley ML, Burian H, Black SE. 2003. Evidence from functional neuroimaging of a compensatory prefrontal network in Alzheimer's disease. J Neurosci 23(3):986–93.

Greicius MD, Srivastava G, Reiss AL, Menon V. 2004. Default-mode network activity distinguishes Alzheimer's disease from healthy aging: evidence from functional MRI. Proc Natl Acad Sci U S A 101(13):4637–42.

Hagmann P, Cammoun L, Gigandet X, Meuli R, Honey CJ, Wedeen VJ, and others. 2008. Mapping the structural core of human cerebral cortex. PLoS Biol 6(7):e159.

Hagmann P, Kurant M, Gigandet X, Thiran P, Wedeen VJ, Meuli R, and others. 2007. Mapping human whole-brain structural networks with diffusion MRI. PLoS ONE 2(7):e597.

He Y, Chen Z, Evans A. 2008. Structural insights into aberrant topological patterns of large-scale cortical networks in Alzheimer's disease. J Neurosci 28(18):4756–66.

He Y, Chen Z, Rosa P, Germann J, Evans A. 2007. Small-world human brain volumetric network revealed by structural MRI. Proceedings of the 13th International Conference on Functional Mapping of the Human Brain, Chicago, Illinois.

He Y, Chen ZJ, Evans AC. 2007. Small-world anatomical networks in the human brain revealed by cortical thickness from MRI. Cereb Cortex 17(10):2407–19.

He Y, Dagher A, Chen Z, Charil A, Zijdenbos A, Worsley K, and others. 2009. White matter lesions impair small-world efficiency in structural cortical networks in multiple sclerosis. Brain. In press.

He Y, Wang L, Zang Y, Tian L, Zhang X, Li K, and others. 2007. Regional coherence changes in the early stages of Alzheimer's disease: a combined structural and resting-state functional MRI study. Neuroimage 35(2):488–500.

Horwitz B, Grady CL, Schlageter NL, Duara R, Rapoport SI. 1987. Intercorrelations of regional cerebral glucose metabolic rates in Alzheimer's disease. Brain Res 407(2):294–306.

Horwitz B, McIntosh AR, Haxby JV, Furey M, Salerno JA, Schapiro MB, and others. 1995. Network analysis of PET-mapped visual pathways in Alzheimer type dementia. Neuroreport 6(17):2287–92.

Iturria-Medina Y, Sotero RC, Canales-Rodriguez EJ, Aleman-Gomez Y, Melie-Garcia L. 2008. Studying the human brain anatomical network via diffusion-weighted MRI and Graph Theory. Neuroimage 40(3):1064–76.

Jelic V, Shigeta M, Julin P, Almkvist O, Winblad B, Wahlund LO. 1996. Quantitative electroencephalography power and coherence in Alzheimer's disease and mild cognitive impairment. Dementia 7(6):314–23.

Kaiser M, Hilgetag CC. 2004. Edge vulnerability in neural and metabolic networks. Biol Cybern 90(5):311–7.

Kaiser M, Hilgetag CC. 2006. Nonoptimal component placement, but short processing paths, due to long-distance projections in neural systems. PLoS Comput Biol 2(7):e95.

Kim JS, Singh V, Lee JK, Lerch J, Ad-Dab'bagh Y, MacDonald D, and others. 2005. Automated 3-D extraction and evaluation of the inner and outer cortical surfaces using a Laplacian map and partial volume effect classification. Neuroimage 27(1):210–21.

Knott V, Mohr E, Mahoney C, Ilivitsky V. 2000. Electroencephalographic coherence in Alzheimer's disease: comparisons with a control group and population norms. J Geriatr Psychiatry Neurol 13(1):1–8.

Koenig T, Prichep L, Dierks T, Hubl D, Wahlund LO, John ER, and others. 2005. Decreased EEG synchronization in Alzheimer's disease and mild cognitive impairment. Neurobiol Aging 26(2):165–71.

Kukull WA, Bowen JD. 2002. Dementia epidemiology. Med Clin North Am 86(3):573–90.

Latora V, Marchiori M. 2001. Efficient behavior of small-world networks. Phys Rev Lett 87(19):198701.

Le Bihan D. 2003. Looking into the functional architecture of the brain with diffusion MRI. Nat Rev Neurosci 4(6):469–80.

Lerch JP, Pruessner JC, Zijdenbos A, Hampel H, Teipel SJ, Evans AC. 2005. Focal decline of cortical thickness in Alzheimer's disease identified by computational neuroanatomy. Cereb Cortex 15(7):995–1001.

Lerch JP, Worsley K, Shaw WP, Greenstein DK, Lenroot RK, Giedd J, and others. 2006. Mapping anatomical correlations across cerebral cortex (MACACC) using cortical thickness from MRI. Neuroimage 31(3):993–1003.

Liu Y, Liang M, Zhou Y, He Y, Hao Y, Song M, and others. 2008. Disrupted small-world networks in schizophrenia. Brain 131(Pt 4):945–61.

MacDonald D, Kabani N, Avis D, Evans AC. 2000. Automated 3-D extraction of inner and outer surfaces of cerebral cortex from MRI. Neuroimage 12(3):340–56.

Maguire EA, Gadian DG, Johnsrude IS, Good CD, Ashburner J, Frackowiak RS, and others. 2000. Navigation-related structural change in the hippocampi of taxi drivers. Proc Natl Acad Sci U S A 97(8):4398–403.

Mechelli A, Friston KJ, Frackowiak RS, Price CJ. 2005. Structural covariance in the human cortex. J Neurosci 25(36):8303–10.

Mentis MJ, Horwitz B, Grady CL, Alexander GE, VanMeter JW, Maisog JM, and others. 1996. Visual cortical dysfunction in Alzheimer's disease evaluated with a temporally graded "stress test" during PET. Am J Psychiatry 153(1):32–40.

Micheloyannis S, Pachou E, Stam CJ, Breakspear M, Bitsios P, Vourkas M, and others. 2006. Small-world networks and disturbed functional connectivity in schizophrenia. Schizophr Res 87(1-3):60–6.

Micheloyannis S, Pachou E, Stam CJ, Vourkas M, Erimaki S, Tsirka V. 2006. Using graph theoretical analysis of multi channel EEG to evaluate the neural efficiency hypothesis. Neurosci Lett 402(3):273–7.

Mori S, van Zijl PC. 2002. Fiber tracking. Principles and strategies: a technical review. NMR Biomed 15(7-8):468–80.

Morrison J, Scherr S, Lewis D, Campbell M, Bloom F, Rogers J. 1986. The laminar and regional distribution of neocortical somatostatin and neuritic plaques: implications for Alzheimer's disease as a global neocortical disconnection syndrome. In: Scheibel A, Wechsler A, and Brazier M (eds.), The Biological Substrates of Alzheimer's Disease. Orlando: Academic Press, 115–31.

Newman ME, Girvan M. 2004. Finding and evaluating community structure in networks. Phys Rev E Stat Nonlin Soft Matter Phys 69(2 Pt 2):026113.

Newman MEJ. 2003. The structure and function of complex networks. SIAM Rev 45(2):167–256.

Parker GJ, Alexander DC. 2005. Probabilistic anatomical connectivity derived from the microscopic persistent angular structure of cerebral tissue. Philos Trans R Soc Lond B Biol Sci 360(1457):893–902.

Pijnenburg YA, v d Made Y, van Cappellen van Walsum AM, Knol DL, Scheltens P, Stam CJ. 2004. EEG synchronization likelihood in mild cognitive impairment and Alzheimer's disease during a working memory task. Clin Neurophysiol 115(6):1332–9.

Prvulovic D, Hubl D, Sack AT, Melillo L, Maurer K, Frolich L, and others. 2002. Functional imaging of visuospatial processing in Alzheimer's disease. Neuroimage 17(3):1403–14.

Raichle ME, MacLeod AM, Snyder AZ, Powers WJ, Gusnard DA, Shulman GL. 2001. A default mode of brain function. Proc Natl Acad Sci U S A 98(2):676–82.

Rose SE, Chen F, Chalk JB, Zelaya FO, Strugnell WE, Benson M, and others. 2000. Loss of connectivity in Alzheimer's disease: an evaluation of white matter tract integrity with colour coded MR diffusion tensor imaging. J Neurol Neurosurg Psychiatry 69(4):528–30.

Rubinov M, Knock SA, Stam CJ, Micheloyannis S, Harris AW, Williams LM, and others. 2007. Small-world properties of nonlinear brain activity in schizophrenia. Hum Brain Mapp.

Salmon E, Lekeu F, Bastin C, Garraux G, Collette F. 2008. Functional imaging of cognition in Alzheimer's disease using positron emission tomography. Neuropsychologia 46(6):1613–23.

Salvador R, Suckling J, Coleman MR, Pickard JD, Menon D, Bullmore E. 2005. Neurophysiological architecture of functional magnetic resonance images of human brain. Cereb Cortex 15(9):1332–42.

Singh V, Chertkow H, Lerch JP, Evans AC, Dorr AE, Kabani NJ. 2006. Spatial patterns of cortical thinning in mild cognitive impairment and Alzheimer's disease. Brain 129(Pt 11):2885–93.

Smit DJ, Stam CJ, Posthuma D, Boomsma DI, de Geus EJ. 2008. Heritability of "small-world" networks in the brain: a graph theoretical analysis of resting-state EEG functional connectivity. Hum Brain Mapp 29(12):1368–78.

Sorg C, Riedl V, Muhlau M, Calhoun VD, Eichele T, Laer L, and others. 2007. Selective changes of resting-state networks in individuals at risk for Alzheimer's disease. Proc Natl Acad Sci U S A 104(47):18760–5.

Sporns O, Chialvo DR, Kaiser M, Hilgetag CC. 2004. Organization, development and function of complex brain networks. Trends Cogn Sci 8(9):418–25.

Sporns O, Tononi G, Kotter R. 2005. The human connectome: A structural description of the human brain. PLoS Comput Biol 1(4):e42.

Stahl R, Dietrich O, Teipel S, Hampel H, Reiser MF, Schoenberg SO. 2003. [Assessment of axonal degeneration on Alzheimer's disease with diffusion tensor MRI]. Radiologe 43(7):566–75.

Stam CJ. 2004. Functional connectivity patterns of human magnetoencephalographic recordings: a 'small-world' network? Neurosci Lett 355(1-2):25–8.

Stam CJ, de Haan W, Daffertshofer A, Jones BF, Manshanden I, van Cappellen van Walsum AM, and others. 2009. Graph theoretical analysis of magnetoencephalographic functional connectivity in Alzheimer's disease. Brain 132(Pt 1):213–24.

Stam CJ, Jones BF, Manshanden I, van Cappellen van Walsum AM, Montez T, Verbunt JP, and others. 2006. Magnetoencephalographic evaluation of resting-state functional connectivity in Alzheimer's disease. Neuroimage 32(3):1335–44.

Stam CJ, Jones BF, Nolte G, Breakspear M, Scheltens P. 2007. Small-world networks and functional connectivity in Alzheimer's disease. Cereb Cortex 17(1):92–9.

Stam CJ, Reijneveld JC. 2007. Graph theoretical analysis of complex networks in the brain. Nonlinear Biomed Phys 1(1):3.

Supekar K, Menon V, Rubin D, Musen M, Greicius MD. 2008. Network analysis of intrinsic functional brain connectivity in Alzheimer's disease. PLoS Comput Biol 4(6):e1000100.

Thompson PM, Cannon TD, Narr KL, van Erp T, Poutanen VP, Huttunen M, and others. 2001. Genetic influences on brain structure. Nat Neurosci 4(12):1253–8.

Thompson PM, Hayashi KM, de Zubicaray G, Janke AL, Rose SE, Semple J, and others. 2003. Dynamics of gray matter loss in Alzheimer's disease. J Neurosci 23(3):994–1005.

Ukmar M, Makuc E, Onor ML, Garbin G, Trevisiol M, Cova MA. 2008. Evaluation of white matter damage in patients with Alzheimer's disease and in patients with mild cognitive impairment by using diffusion tensor imaging. Radiol Med 113(6):915–22.

Wada Y, Nanbu Y, Koshino Y, Yamaguchi N, Hashimoto T. 1998. Reduced interhemispheric EEG coherence in Alzheimer disease: analysis during rest and photic stimulation. Alzheimer Dis Assoc Disord 12(3):175–81.

Wakana S, Jiang H, Nagae-Poetscher LM, van Zijl PC, Mori S. 2004. Fiber tract-based atlas of human white matter anatomy. Radiology 230(1):77–87.

Wang J, Wang L, Zang Y, Yang H, Tang H, Gong Q, and others. 2009. Parcellation-dependent small-world brain functional networks: a resting-state fMRI study. Hum Brain Mapp 30(5):1511-23.

Wang K, Liang M, Wang L, Tian L, Zhang X, Li K, and others. 2007. Altered functional connectivity in early Alzheimer's disease: a resting-state fMRI study. Hum Brain Mapp 28(10):967–78.

Wang L, Zang Y, He Y, Liang M, Zhang X, Tian L, and others. 2006. Changes in hippocampal connectivity in the early stages of Alzheimer's disease: evidence from resting state fMRI. Neuroimage 31(2):496–504.

Wang L, Zhu C, He Y, Zang Y, Cao Q, Zhang H, and others. 2009. Altered small-world brain functional networks in children with attention-deficit/hyperactivity disorder. Hum Brain Mapp 30(2):638-49.

Watts DJ, Strogatz SH. 1998. Collective dynamics of 'small-world' networks. Nature 393(6684):440–2.

Wright IC, Sharma T, Ellison ZR, McGuire PK, Friston KJ, Brammer MJ, and others. 1999. Supra-regional brain systems and the neuropathology of schizophrenia. Cereb Cortex 9(4):366–78.

Xie S, Xiao JX, Gong GL, Zang YF, Wang YH, Wu HK, and others. 2006. Voxel-based detection of white matter abnormalities in mild Alzheimer disease. Neurology 66(12):1845–9.

For reprints and permissions queries, please visit SAGE's Web site at http://www.sagepub.com/journalsPermissions.nav.